A High Efficiency/Output Power and Low Noise Megahertz Wireless Power Transfer System over A Wide Range of Mutual Inductance

Ming Liu, *Student Member, IEEE,* Shuangke Liu, *Student Member, IEEE,* Chengbin Ma, *Member, IEEE*

Abstract—**Wireless power transfer (WPT) systems working at several megahertz (MHz) are widely considered as a promising solution for a mid-range transfer of a medium amount of power. The soft-switching based Class E power amplifier (PA) and rectifier are known to be suitable for high frequency applications, which may potentially improve the performance of the MHz WPT systems. Meanwhile, the efficiency and output power of the Class E PA is sensitive to its loading condition, particularly when there is variation in the relative position of the coupling coils, namely a changed mutual inductance between the coils. Thus the purpose of this paper is to propose and discuss circuit and design improvements that maintain a high efficiency and output power of the MHz WPT systems over a wide range of mutual inductance, when the Class E PA and rectifier are employed. Besides, the suppression of the harmonic contents, i.e., the electromagnetic interference problem, is also taken into account in the circuit design. Both the simulation and experimental results show that the newly added and optimally designed π matching network obviously improves the drops of the efficiency and output power of the Class E PA and the overall WPT system when the mutual inductance varies. The reduction of the total harmonic distortion in the input voltage of the coupling coils is also significant, from the original 52.9% to 9.6%. The circuit and design improvements discussed in this paper could serve as a general and practical solution for building high performance MHz WPT systems.**

Index Terms—**Megahertz wireless power transfer, matching network, efficiency, output power, harmonics**

I. Introduction

WIRELESS power transfer (WPT) is receiving considerable attention from both academia and industry due to a dramatic need to wirelessly charge various electronic devices (e.g., cellphones, laptop computers, wearable devices, medical implant devices, etc.) and the systems requiring much higher power (e.g., electric vehicles and robots). Now the near-field WPT is popular such as through the inductive resonance coupling working at either kilohertz (kHz) or several megahertz (MHz), 6.78 and 13.56 MHz at ISM (industrial,

M. Liu, S. Liu, and C. Ma are with the University of Michigan-Shanghai Jiao Tong University Joint Institute, Shanghai Jiao Tong University, No. 800 Dongchuan Road, Shanghai 200240, China (e-mail: mikeliu@sjtu.edu.cn; liushuangke@sjtu.edu.cn; chbma@sjtu.edu.cn).

scientific, and medical) band [1]. The kHz WPT systems are particularly superior for high power applications thanks to the new development of power electronics [2]–[7]. Meanwhile, in terms of spatial freedom, namely a longer transfer distance and higher tolerance to coupling coil misalignment, the WPT at MHz is advantageous. Besides, higher the operating frequency, more compact and lighter a WPT system [8], [9]. These aspects are especially useful for mid-range and low power applications such as charging a consumer electronic device. Efforts have been made to build high efficiency MHz WPT systems through compensation of coils, high efficiency power amplifiers (PAs) and rectifiers, tunable circuit, frequency tunning, optimal load tracking, etc [10]–[15].

A practical challenge for MHz WPT is the high switching loss when using conventional hard-switching based PAs and rectifiers such as the full-bridge ones. Recently, the soft-switching based ones have begun to be applied in the WPT systems, particularly the MHz WPT systems [16]–[20]. For instance, the Class E PA and rectifier were originally developed for general high frequency applications thanks to their soft-switching properties. Using the Class E half-wave rectifier in WPT was first investigated in [17]. A high efficiency of the rectifier, 94.43%, was reported when working at 800 kHz. [20] developed a system-level optimization procedure for a 6.78-MHz WPT system, which used both a Class E PA and a Class E half-wave rectifier, i.e., a so-called Class E^2 dc-dc converter. An 84% dc-to-dc efficiency was achieved with loosely coupled coils (mutual inductance coefficient k=0.1327) and at a power level of 20 W. In such systems, the performance of the Class E PA is important for providing a high efficiency and output power of the overall MHz WPT system. This type of PA is known to be a promising high-frequency ac power source due to its simple topology and zero-voltage switching (ZVS)/zero-voltage-derivation switching (ZVDS) properties [21]. Meanwhile, difficulties arise from the uncertainties such as possible variation in the relative position of the coupling coils (i.e., the mutual inductance), which could be common in real applications. This problem is especially challenging for a WPT system driven by a Class E PA due to the high load sensitivity of the PA [19]. The Class E PA using a finite (ac) choke has been investigated to improve PA efficiency under a varying PA load [22], [23]. However, its design solution cannot be analytically represented, which makes it difficult to perform optimized parameter design. Thus this paper focuses on Class E PA using an infinite (dc) choke. Besides, it should also be noted that another potential problem is the

electromagnetic interference (EMI). This issue is particularly crucial for building a practical WPT system working at MHz. As to the knowledge of the authors, there are few discussions in the literature so far on suppressing the harmonic contents in MHz WPT systems.

Various adaptive approaches have been developed to improve performance of WPT systems, mostly system efficiency, when operating in dynamic environments. Operating frequency, matching network before transmitting coil and/or after receiving coil, and dc-dc converter after rectifier can be adaptively tuned or controlled to maximize the efficiency in different coil relative positions and with a changing load, i.e., adaptive frequency tuning, adaptive impedance matching, and adaptive rectification, respectively [12]. The adaptive frequency tuning achieves high efficiency when the transmitting and receiving coils are overcoupled [24]. However, it may violate regulations by operating outside the narrow 6.78 or 13.56-MHz band. Adaptive impedance matching is considered to be a more practical solution. For example, matching capacitor values can be determined that maximize the efficiency, such as through simulation at each coil relative position. On the other hand, the requirement on tunable components (e.g. variable capacitors and/or inductors) complicates its design and real implementation [16], [25]. A dc-dc converter can also be added between the rectifier and final load, and controlled to provide an optimal load seen by the rectifier [12]. The dc-dc converter minimizes the effect of a dynamic load to the system efficiency, and helps to alleviate the need of the adaptive impedance matching. In the above adaptive approaches, besides relatively complicated control algorithms, dedicated hardware is required to measure, communicate, calculate, and implement the control. This further increases system complexity. For many real applications, a simplified solution such as static impedance matching is usually more preferred that improves reliability and cost-performance. In addition, in most cases there are multiple design objectives (high efficiency, high output power, low noise, etc.) required by a practical WPT system. However, there is a lack of discussions on a design methodology for such a robust and high-performance WPT system.

Based on the above considerations, this paper discusses and proposes improvements on the circuit and the design methodology. The purpose is to provide a systematic solution that enables not only high efficiency but also high output power and low noise MHz WPT systems. Most existing MHz WPT systems employ hard-switching-based rectifiers such as a full-bridge rectifier. The hard-switching operation at MHz causes significant switching loss, and also leads to high voltage harmonic contents, namely a high total harmonic distortion (THD), in WPT systems because of the square-wave input voltage in the full-bridge rectifier. In this paper, a soft-switching-based Class E full-wave rectifier is applied. Thanks to its sinusoidal input voltage and current, this rectifier yields low switching loss and low switching noise, i.e., a low THD in the input voltage of the rectifier [26]. Note that the two parallel capacitors of the full-wave rectifier need to be delicately designed to achieve maximized performance. Care should also be taken to avoid high voltage stress on rectifying

diodes. A π matching network is further added between the Class E PA and the coupling coils. This matching network performs load transformation that maintains the load of the PA within a desired region for high efficiency and high output power when the mutual inductance varies. An additional constraint is also added on determining the matching capacitor values. Its purpose is to reduce the input voltage THD of the coupling coils. A new system-level design methodology is then developed to calculate a set of fixed matching capacitor values, namely static impedance matching, that enables the matching network to simultaneously perform the load transformation and suppression of the harmonic contents in dynamic environments.

This paper is thus organized as follows. Section II reviews the conventional design of a MHz WPT system using both the Class E PA and full-wave rectifier. The efficiency and the output power of the Class E PA significantly drop under different mutual inductances, and a high THD is also observed in the input voltage of the coupling coils. Section III discusses the improvements in circuit and the design methodology. The input impedance of the coupling coils is analytically derived. It helps to optimally determine the design parameters of the π matching network that transforms the load of the PA within its desired range and minimizes the harmonic contents. Then, section IV validates the analytical and design results by real experiments using an example 6.78-MHz WPT system. Finally, section V draws the conclusion.

II. REVIEW OF CONVENTIONAL DESIGN

Fig. 1 shows the circuit model of a 6.78-MHz WPT system. It consists of a Class E PA, two coupling coils, and a Class E full-wave rectifier. Z_{in} and Z_{rec} are the input impedances of the coupling coils and the Class E full-wave rectifier, respectively. P_{dc} is the dc input power of the Class E PA; $P_{Z_{\text{in}}}$ is the input power of the coupling coils; P_{rec} is the input power of the rectifier; and P_o is the dc output power of the rectifier. V_{dc} is the dc input voltage of the PA. $v_{Z_{\text{in}}}$ and $i_{Z_{\text{in}}}$ are the input voltage and current of the coupling coils, respectively. Similarly, v_{rec} and i_{rec} are the input voltage and current of the rectifier, respectively. In the circuit model, C_S, C_0, C_{tx}, C_{rx}, and C (=C_1=C_2) are the design parameters of the WPT system and other parameters are constant ones. Here C_{tx} and C_{rx} are the compensation capacitors of the transmitting and receiving coils, respectively.

In conventional design, the design parameters are optimized as follows. First, in order to avoid the overlapping of diode conduction and lower diode voltage stress, C, namely C_1 and C_2, is determined to enable a duty cycle D smaller than 0.5 (here 0.45) for the two rectifying diodes, D_1 and D_2 [26]. Then, taking the reactance of Z_{rec} into consideration, C_{rx} is designed to achieve full resonance of the receiving coil, and C_{tx} is selected to resonate with the transmitting coil. Thus a pure resistive Z_{in}, the PA load, is achieved under specific mutual inductance coefficient (k) and dc load (R_L). Finally, the PA design parameters, C_0 and C_S, are designed to achieve ZVS through following equations [27],

$$C_S = \frac{0.1836}{\omega Z_{\text{in}}}, \qquad (1)$$
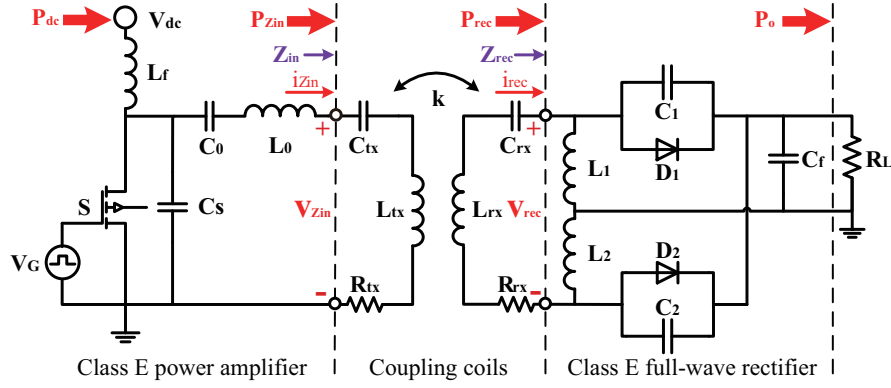
Fig. 1. Circuit model of a 6.78-MHz WPT system using Class E PA and Class E full-wave rectifier.

$$C_0 = \frac{1}{\omega^2 L_0 - 1.1525\omega Z_{\mathrm{in}}}. \tag{2}$$

Following these requirements, the optimized design parameters are calculated and listed in Table I for a fixed mutual inductance coefficient k (=0.2) and an example dc load R_L (=30 Ω). The performance of the 6.78-MHz WPT system in Fig. 1 is then investigated using a well-known RF circuit simulation software, Keysight ADS. The simulation uses the Pspice models of the diode, STPSC406, and the MOSFET, SUD06N10. Besides the design parameters, the constant parameters, the inductances and the equivalent series resistances (ESRs) of the components, in the simulation are also listed in Table II. L_0 is the series inductor of the conventional Class E PA matching network. The series combination of L_0 and C_0 determines the PA load reactance. A large L_0 helps to achieve close-to-sinusoidal PA output current, but leads to high power loss due to its large ESR. As shown in Table II, in this paper a 1.465 μH L_0 is chosen, whose ESR is 0.2 Ω at 6.78 MHz. Note that L_f, L_1, and L_2 are dc filter inductors. Their inductances should be sufficiently large such that the ac current will not flow through them.

TABLE I
OPTIMAL DESIGN PARAMETERS WITH A FIXED k.

C_S	C_0	C_{tx}	C_{rx}	C	D
262 pF	540 pF	165 pF	326 pF	202 pF	0.45

TABLE II
CONSTANT PARAMETERS

L_f	L_0	L_{tx}	L_{rx}	L_1/L_2
68 μH	1.465 μH	3.34 μH	3.34 μH	68 μH
r_{L_f}	r_{L_0}	r_{tx}	r_{rx}	r_{L_1}/r_{L_2}
0.2 Ω	0.2 Ω	0.8 Ω	0.8 Ω	0.2 Ω

Fig. 2(a) gives the efficiency of the Class E PA versus different k's varying between 0.14 and 0.44. Here the PA efficiency is defined as the ratio of $P_{Z_{\mathrm{in}}}$ to P_{dc}. The Class E PA achieves a very high efficiencies, 94%, under the target k (=0.2). However, its efficiency significantly drops when k deviates from its target value, which inevitably leads to a low system efficiency. Similar trend of the PA output power

can also be observed, as shown in Fig. 2(b). It is because the varying k leads to changes in PA load, Z_{in}. Thus, the Class E PA deviates from its ZVS operation, which lowers PA efficiency and system efficiency. This aspect will be further explored in section III-B.
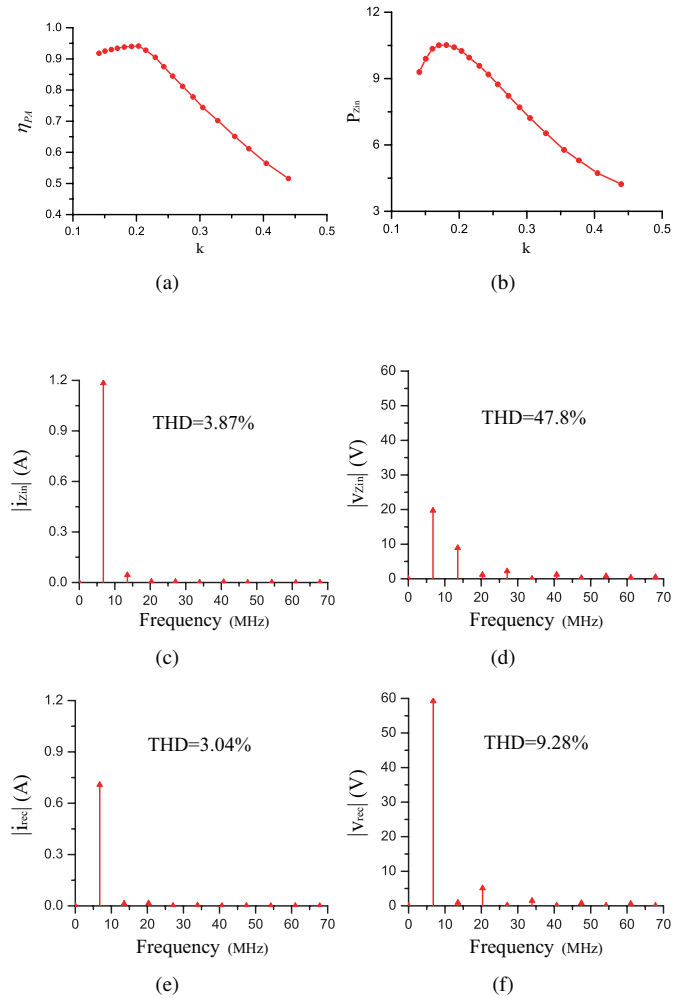
Fig. 2. Simulation results. (a) Efficiency of PA. (b) Output power of PA. (c) Harmonic contents in $i_{Z_{\mathrm{in}}}$. (d) Harmonic contents in $v_{Z_{\mathrm{in}}}$. (e) Harmonic contents in i_{rec}. (f) Harmonic contents in v_{rec}

It is known that the input/output voltage/current harmonic
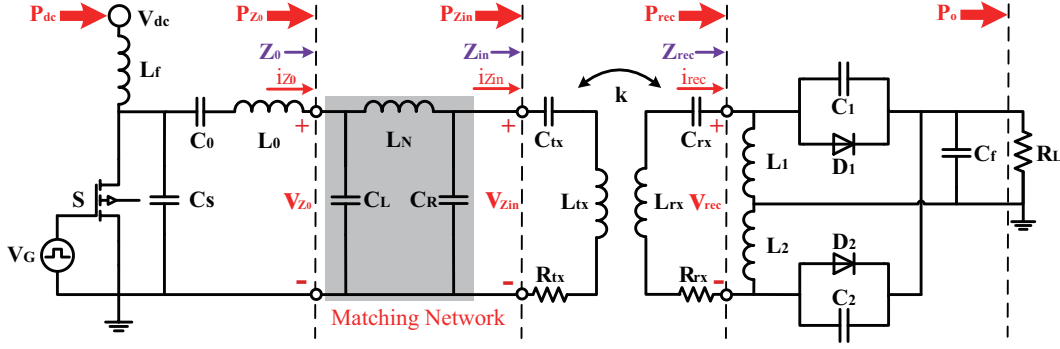
Fig. 3. Circuit model of the improved 6.78-MHz WPT system with an additional π matching network.

contents of coupling coils, i.e., the harmonic contents in $v_{Z_{\mathrm{in}}}$, $i_{Z_{\mathrm{in}}}$, v_{rec}, and i_{rec}, may lead to a severe EMI problem. Thus it is important to suppress the harmonic contents of the coupling coils, especially for MHz WPT systems. In the WPT system shown in Fig. 1, ideally the input current, $i_{Z_{\mathrm{in}}}$, and the output current, i_{rec}, of the coupling coils are sinusoidal because the coils are series-series resonant ones. This explains the low harmonic contents in $i_{Z_{\mathrm{in}}}$ and i_{rec}, as shown by their total THDs in Fig. 2(c) and (e). Here the definition of THD is given as follows using $i_{Z_{\mathrm{in}}}$ as an example,

$$\mathrm{THD} = \frac{\sqrt{\sum_{n=2}^{\infty} i^2_{Z_{\mathrm{in}},n}}}{i_{Z_{\mathrm{in}},1}}, \tag{3}$$

where $i_{Z_{\mathrm{in}},1}$ is the fundamental component of the input current of the coupling coils at the resonant frequency, 6.78 MHz here, and $i_{Z_{\mathrm{in}},n}$ represents the n-order input current harmonic. By using the Class E full-wave rectifier, the output voltage of coupling coils, v_{rec}, is also sinusoidal, and thus its THD is low [see Fig. 2(f)]. However, as show in Fig. 2(d), the THD of $v_{Z_{\mathrm{in}}}$ is high, 47.8%, particularly due to the second-order harmonic. The suppression of this second-order harmonic in $v_{Z_{\mathrm{in}}}$ is discussed in the following section.

III. Circuit and Design Improvements

As explained above, the conventional design only guarantees an optimized performance of the Class E PA, such as its efficiency and output power, under a fixed mutual inductance coefficient, k. However, in real applications it is usually common that the relative position of the coupling coils changes, i.e., a varying k. This may obviously deteriorate the original performance of the PA and the overall WPT system, as shown in Fig. 2. In addition, a high THD in the input voltage of the coupling coils, $v_{Z_{\mathrm{in}}}$, is observed, particularly due to the second-order harmonic. In order to maintain high efficiency and output power of the Class E PA over a wide range of k and suppress the harmonic contents, improvements on the circuit and the design are required.

As shown in Fig. 3, a π matching network is added to the original 6.78-MHz WPT system. The matching network separates the Class E PA and the following circuits. It brings new design freedom, C_L and C_R specifically, that makes the further optimization possible considering a varying k. In the

following subsections, the input impedance of the coupling coils, Z_{in}, is analytically derived that helps to calculate the load of the PA, i.e., the input impedance of the matching network, in the improved WPT system. The purpose of the π matching network is to transform the PA load into a desired range for high efficiency and output power when Z_{in} varies due to a changed k. The candidate C_L's and C_R's, the two design parameters of the matching network, are determined accordingly for the required load transform. The final pair of C_L and C_R is the one that minimizes the second-order harmonic in the input voltage of the coupling coils, $v_{Z_{\mathrm{in}}}$.

A. Input Impedance of Coupling Coils

As mentioned above, it is important to first derive the relationship between Z_{in} and k, for the following parameter design of the matching network. As shown in Fig. 3, the Class E full-wave rectifier consists of two filter inductors, L_1 and L_2, two parallel capacitors, C_1 and C_2 with an identical capacitance C, two rectifying diodes, D_1 and D_2, and a filter capacitor C_o. As discussed in [26], in order to avoid the overlapping of the diode conduction and thus the hard switching, the duty cycle D of the rectifier should be smaller than 0.5. Here D is chosen as 0.45, as same as the one in the conventional design. Again from [26] and using the parameters, D (=0.45) and C (=202 pF), in table I, the input impedance of the rectifier, Z_{rec} (=$R_{\mathrm{rec}} + jX_{\mathrm{rec}}$), can be calculated as

$$R_{\mathrm{rec}} = 1.694 R_L \ , \tag{4}$$

and

$$X_{\mathrm{rec}} = -2.344 R_L \ , \tag{5}$$

where R_L is the dc load.
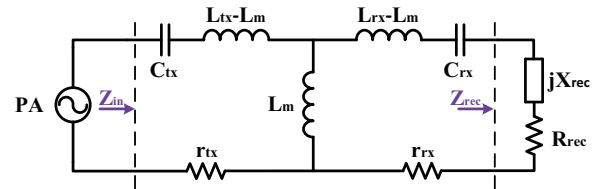
Fig. 4. Equivalent circuit model of the coupling coils.

Fig. 4 shows an equivalent circuit model of the series-series resonant coupling coils in the 6.78-MHz WPT system. In the

figure, the Class E full-wave rectifier is represented by its input impedance, Z_{rec}. L_{tx} and L_{rx} are the inductances of the transmitting and receiving coils, respectively. C_{tx} and C_{rx} are the compensation capacitors. r_{tx} and r_{rx} are the ESRs of L_{tx} and L_{rx}, respectively. L_m is the mutual inductance,

$$L_m = k\sqrt{L_{\text{tx}}L_{\text{rx}}}. \tag{6}$$

It is well-known that the resonance can improve the efficiency and power transfer capacity of the coupling coils [8]. Due to the existence of the non-zero X_{rec}, C_{tx} and C_{rx} should be designed following the below equations that make the two coils exactly resonant,

$$j\omega L_{\text{rx}} + \frac{1}{j\omega C_{\text{rx}}} + jX_{\text{rec}} = 0, \tag{7}$$

$$j\omega L_{\text{tx}} + \frac{1}{j\omega C_{\text{tx}}} = 0, \tag{8}$$

where ω is the target resonant frequency, 6.78 MHz here. From Fig. 4 and the conditions of (7) and (8), the input impedance of the coupling coils, Z_{in}, can be expressed as

$$Z_{\text{in}} = R_{Z_{\text{in}}} + jX_{Z_{\text{in}}} = r_{\text{tx}} + \frac{\omega^2 k^2 L_{\text{tx}}L_{\text{rx}}}{r_{\text{rx}} + R_{\text{rec}}}, \tag{9}$$

where $R_{Z_{\text{in}}}$ and $X_{Z_{\text{in}}}$ are the resistance and reactance of Z_{in}, respectively. Note Z_{in} is pure resistive because the non-zero X_{rec} is fully compensated by C_{rx} on the receiving side, and R_{rec} is 1.694 times of R_L [refer to (4)(7)]

B. Target Region and Harmonic Suppression

In the present MHz WPT system, the Class E PA drives the coupling coils. As shown in Fig. 3, the PA consists of a dc voltage supply V_{dc}, a dc filter inductor L_f, a MOSFET switch S, a shunt capacitor C_S, a series capacitor C_0, and a series inductor L_0. Usually C_S and C_0 are the design parameters for the Class E PA, and again L_f should be sufficiently large. Based on the PA circuit model and the parameters in Table I and II, the efficiency and output power contours of the Class E PA are given in Fig. 5 through sweeping the equivalent resistance and reactance of the load of the PA, i.e., Z_0 ($=R_0 + jX_0$) in Fig. 3. Note Z_0 simply equals Z_{in} if there is no matching network. Here the dc input voltage of the PA is 20 V. Meanwhile, the results in Fig. 5 are general for other dc input voltages within the permissible range. The pure resistive Z_{in}, i.e., $R_{Z_{\text{in}}}$ in (9), is also shown in the contours when k varies from 0.14 to 0.44. It can be seen that along the vertical lines of $R_{Z_{\text{in}}}$, larger the k, greater the $R_{Z_{\text{in}}}$ and more severe the drops of the efficiency and the output power of the PA, assuming the π matching network is not employed (i.e., $Z_0 = Z_{\text{in}}$). This tendency well explains the simulation results in Fig. 2(a)(b).

As shown in Fig. 5, there is a common region of Z_0, the load of the Class E PA, for both high efficiency and high output power. Thus it would be desirable that the π matching network is designed to transform the load of the PA into this target region when k varies. Here the target region, the rectangular dash lines in Fig. 5(a) and (b), is defined as [-4, 8] for X_0 and [3.8, 31] for R_0 to achieve efficiency and output power of the PA over 85% and 8 W, respectively. As

shown in Fig. 3, the matching network consists of a series inductor, L_N, and two parallel capacitors, C_L and C_R. The capacitors, C_L and C_R, are the design parameters, and L_N is a 390 nH inductor in the present WPT system. The input impedance of the matching network, i.e., Z_0, is analytically derived in (10) and (11), which is determined by Z_{in}, C_L, and C_R. And according to (9), Z_{in} varies with different k. Thus the design of the π matching network depends on the pre-assumed variation range of k and the target region of Z_0 that maintains a high efficiency and output power of the Class E PA.

Besides, it would be desirable that the matching network could also suppress the harmonic contents, particularly the second-order harmonic in $v_{Z_{\text{in}}}$ here, the input voltage of the coupling coils [refer to section II]. The amplitude of $v_{Z_{\text{in}}}$ at the fundamental frequency, 6.78 MHz, $\left|v_{Z_{\text{in}}}^{(1)}\right|$, can be expressed as

$$\left|v_{Z_{\text{in}}}^{(1)}\right| = \left|Z_{\text{in}}^{(1)}\right|\left|i_{Z_{\text{in}}}^{(1)}\right|, \tag{12}$$

where the superscript, "(1)", means a quantity at the fundamental frequency. Note this superscript is neglected in the previous discussions for the sake of simplicity. $\left|i_{Z_{\text{in}}}^{(1)}\right|$ is the amplitude of the input current of the coupling coils, $i_{Z_{\text{in}}}$. Neglecting the power loss in the π matching network gives

$$\frac{\left|i_0^{(1)}\right|^2}{2}R_0^{(1)} = \frac{\left|i_{Z_{\text{in}}}^{(1)}\right|^2}{2}R_{Z_{\text{in}}}^{(1)}, \tag{13}$$

where $|i_0|$ is the amplitude of the input current of the matching network. Thus (12) can be rewritten as

$$\left|v_{Z_{\text{in}}}^{(1)}\right| = \left|Z_{\text{in}}^{(1)}\right|\left|i_0^{(1)}\right|\sqrt{\frac{R_0^{(1)}}{R_{Z_{\text{in}}}^{(1)}}}. \tag{14}$$

Similarly, the amplitude of the second-order harmonic in $v_{Z_{\text{in}}}$, $\left|v_{Z_{\text{in}}}^{(2)}\right|$, can be expressed as

$$\left|v_{Z_{\text{in}}}^{(2)}\right| = \left|Z_{\text{in}}^{(2)}\right|\left|i_0^{(2)}\right|\sqrt{\frac{R_0^{(2)}}{R_{Z_{\text{in}}}^{(2)}}}, \tag{15}$$

where again the superscript, "(2)", means a second-order harmonic. Then the ratio of $\left|v_{Z_{\text{in}}}^{(2)}\right|$ to $\left|v_{Z_{\text{in}}}^{(1)}\right|$, is

$$\frac{\left|v_{Z_{\text{in}}}^{(2)}\right|}{\left|v_{Z_{\text{in}}}^{(1)}\right|} = \frac{\left|Z_{\text{in}}^{(2)}\right|\left|i_0^{(2)}\right|\sqrt{R_{Z_{\text{in}}}^{(1)}}}{\left|Z_{\text{in}}^{(1)}\right|\left|i_0^{(1)}\right|\sqrt{R_{Z_{\text{in}}}^{(2)}}} \cdot \sqrt{\frac{R_0^{(2)}}{R_0^{(1)}}}. \tag{16}$$

A lower second-order harmonic and thus a lower THD in $v_{Z_{\text{in}}}$ can be achieved by having a smaller ratio of $R_0^{(2)}$ to $R_0^{(1)}$ in the WPT system. This requirement on the harmonic suppression is taken into account in the following design of the π matching network.

C. Design of Matching Network

As discussed above, for a high efficiency and output power of the Class E PA and the overall MHz WPT system, it is desired that the values of R_0 and X_0 should be within a

$$R_0 = \frac{\frac{Z_{\text{in}}}{\omega^2 C_L C_R}(\omega L_N - \frac{1}{\omega C_L})(\omega L_N - \frac{1}{\omega C_R}) - \frac{\omega L_N Z_{\text{in}}}{\omega^2 C_L C_R}(\omega L_N - \frac{1}{\omega C_L} - \frac{1}{\omega C_R})}{(\omega L_N Z_{\text{in}} - \frac{Z_{\text{in}}}{\omega C_L} - \frac{Z_{\text{in}}}{\omega C_R})^2 + (\frac{\omega L_N}{\omega C_R} - \frac{1}{\omega^2 C_L C_R})^2}, \tag{10}$$

$$X_0 = -\frac{\frac{Z_{\text{in}}^2}{\omega C_L}(\omega L_N - \frac{1}{\omega C_R})(\omega L_N - \frac{1}{\omega C_L} - \frac{1}{\omega C_R}) + \frac{\omega L_N}{\omega^3 C_L C_R^2}(\omega L_N - \frac{1}{\omega C_L})}{(\omega L_N Z_{\text{in}} - \frac{Z_{\text{in}}}{\omega C_L} - \frac{Z_{\text{in}}}{\omega C_R})^2 + (\frac{\omega L_N}{\omega C_R} - \frac{1}{\omega^2 C_L C_R})^2}, \tag{11}$$
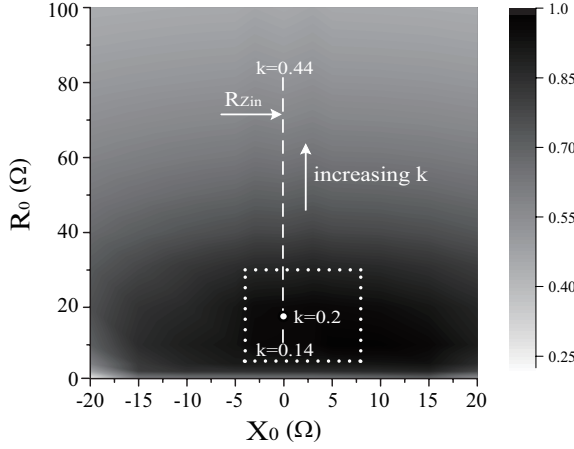
(a)
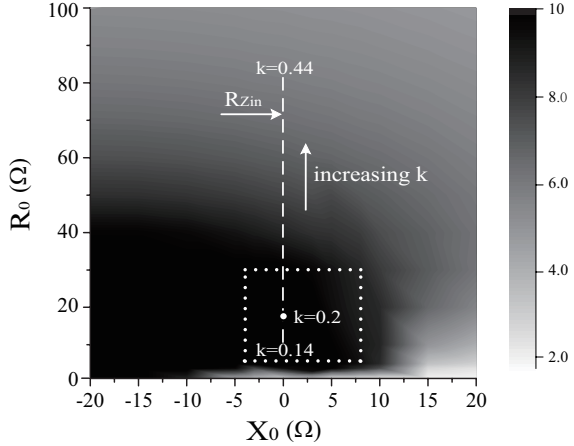
(b)

Fig. 5. Efficiency and output power contours of the Class E PA (Z_0 equals Z_{in} if there is no matching network). (a) Efficiency. (b) Output power (W).

target region. The π matching network can be added after the PA for the required load transformation when k varies. The procedures of determining C_L and C_R, the two design parameters of the matching network, are developed as follows.

First, for implementation purposes, suppose the feasible ranges for selecting C_L and C_R are

$$C_L \in (C_L^{lower}, C_L^{upper}), \tag{17}$$

$$C_R \in (C_R^{lower}, C_R^{upper}), \tag{18}$$

where the superscripts, "$lower$" and "$upper$", mean the lower and upper bounds of a parameter, respectively. For a high efficiency and output power of the Class E PA, its load,

$Z_0^{(1)} = R_0^{(1)} + jX_0^{(1)}$, should be constrained to stay in a desired target region, i.e.,

$$R_0^{lower} \leq R_0^{(1)}(k, C_L, C_R) \leq R_0^{upper}, \tag{19}$$

$$X_0^{lower} \leq X_0^{(1)}(k, C_L, C_R) \leq X_0^{upper}, \tag{20}$$

as explained by Fig. 5(a)(b) and (9)–(11). Besides, the second-order harmonic is the main contributor to the high THD of the input voltage of the coupling coils. From the analysis in the previous section, the ratio of $R_0^{(2)}$ to $R_0^{(1)}$ should be restricted. Again $R_0^{(2)}$ and $R_0^{(1)}$ are the loads of the PA at the second harmonic and fundamental frequencies, respectively. Thus an addition constraint to suppress the second-order harmonic is

$$R_0^{(2)}(k, C_L, C_R) \leq \lambda \cdot R_0^{(1)}(k, C_L, C_R), \tag{21}$$

where λ is an index. Lower λ, smaller the second-order harmonic and THD in the input voltage of the coupling coils. The above constraints together, (17)–(21), define the requirements when designing the π matching network, i.e., the values of C_L and C_R. Since there are only two design parameters, the candidate combinations of the two capacitors can be obtained by simply sweeping C_L and C_R in (10)(11) within their feasible ranges, (17)(18), and confirming if the calculated $R_0^{(1)}$, $X_0^{(1)}$, and $R_0^{(2)}$ meet the constraints in (19)–(21) when k varies. Note Z_{in} in (10)(11) changes with a specific k [refer to (9)]. The final pair of C_L and C_R could be the one with the smallest ratio of $R_0^{(2)}$ to $R_0^{(1)}$, as applied in the following experiments.

IV. EXPERIMENTAL RESULTS

As shown in Fig. 6, the example 6.78-MHz WPT system is built up to validate the above analysis and the design of the π matching network. Its configuration is as same as the circuit model in Fig. 3, and except C_L, C_R, and L_N (=390 nH), the other system parameters are as same as the ones in Table I and II. Here L_N is selected to partly compensate the estimated input reactance of the parallel combination of C_R and the following circuits. Its value, 390 nH, is finalized according to the available commercial products. In the experimental system, STPSC406 SiC diodes are used as the rectifying diodes, D_1 and D_2. The switch of the PA, S, is a SUD06N10 MOSFET. The parasitic capacitors of STPSC406 and SUD06N10 are assumed to be constant, 35 pF and 50 pF, according to their datasheets. Note the parasitic capacitances of D_1, D_2, and S are included in C_1, C_2 (=C), and C_S [refer to Table I]. In the following experiments, the measured input impedance, Z_0, is obtained through the fast Fourier transform (FFT) of the raw data from the oscilloscope. In order to achieve a high-accuracy measurement, the voltage and current probes are calibrated for
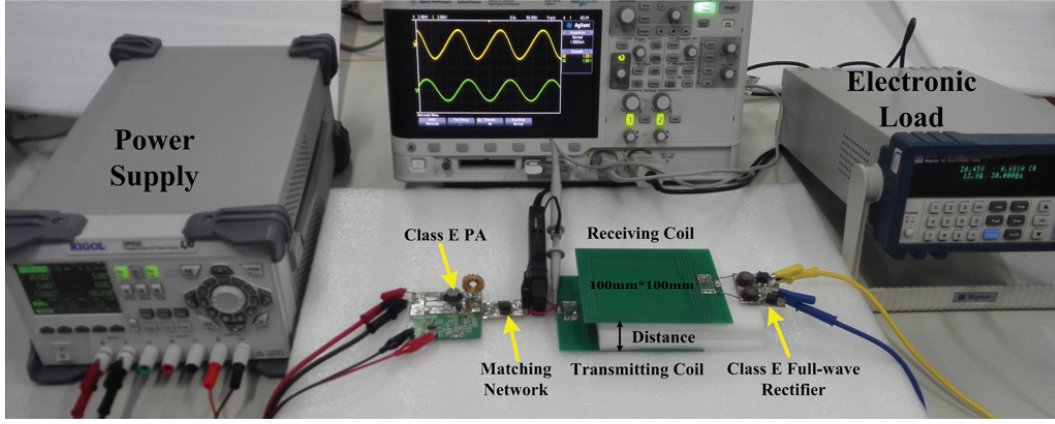
Fig. 6. Experiment setup of the 6.78-MHz WPT system using π matching network.

a same phase at 6.78 MHz. Here the feasible range of the design parameters, C_L and C_R, are given as follows,

$$
\begin{aligned}
(C_L^{lower}, C_L^{upper}) &= (50 \text{ pF}, 2000 \text{ pF}), \\
(C_R^{lower}, C_R^{upper}) &= (50 \text{ pF}, 2000 \text{ pF}).
\end{aligned} \tag{22}
$$

As mentioned in section III-B, the target region for the load of the Class E PA to achieve high efficiency and output power is

$$
\begin{aligned}
(R_0^{lower}, R_0^{upper}) &= (3.8 \ \Omega, 31 \ \Omega), \\
(X_0^{lower}, X_0^{upper}) &= (-4 \ \Omega, 8 \ \Omega).
\end{aligned} \tag{23}
$$

As an example, the index λ in (21) is 0.1 for suppressing the harmonic contents in the input voltage of coupling coils. And the mutual inductance coefficient k is assumed to vary between 0.14 and 0.44 (a coil distance from 40 to 10 mm) [see Fig. 6]. Through the sweeping, the pair of (C_L, C_R) with the smallest ratio of $R_0^{(2)}$ to $R_0^{(1)}$ is determined as

$$
\begin{cases}
C_L = 1150 \text{ pF}, \\
C_R = 1110 \text{ pF}.
\end{cases} \tag{24}
$$

(a) (b)
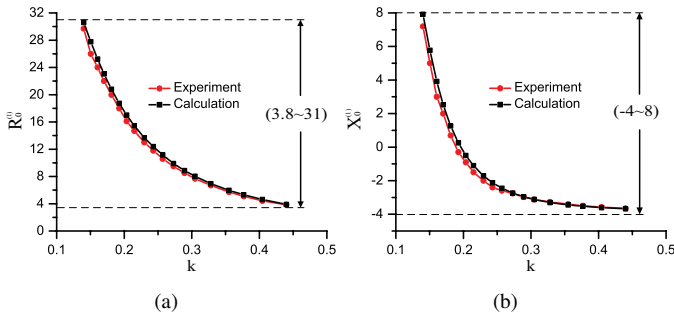
Fig. 7. $Z_0^{(1)}$ versus k. (a) Resistance, $R_0^{(1)}$. (b) Reactance, $X_0^{(1)}$.

Fig. 7 shows the experimental results of the PA load, $Z_0^{(1)}$ ($= R_0^{(1)} + jX_0^{(1)}$), when C_L and C_R in (24) are applied. Through the optimized design of the π matching network, all the values of $R_0^{(1)}$ and $X_0^{(1)}$ are well within the target region defined in (23) when k changes between 0.14 and 0.44. The good matching between the experimental and calculate results

(a) (b)

(c) (d)
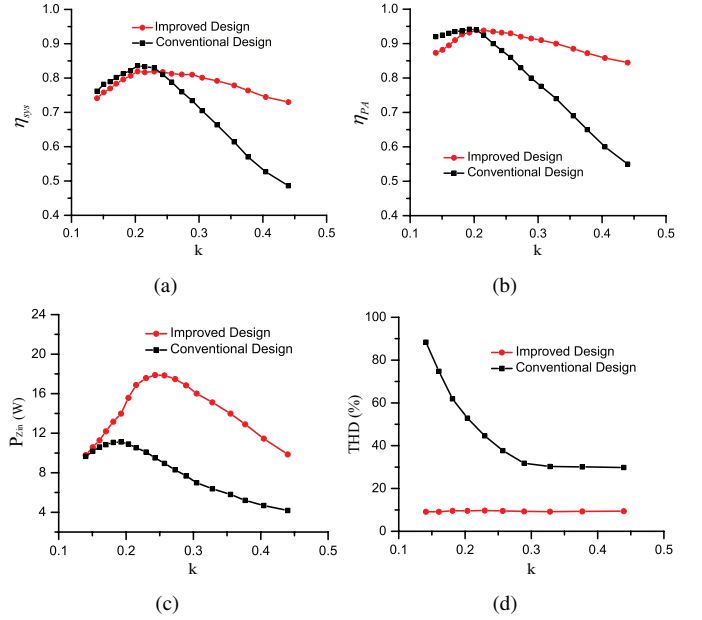
Fig. 8. System and PA efficiencies, PA output power, and THD in the input voltage of the coupling coils under different k. (a) System efficiency. (b) PA efficiency. (c) PA output power. (d) THD in $V_{Z_{in}}$.

also validates the correctness of the analytical derivations in (9)-(11).

Fig. 8(a) and (b) show the system and PA efficiencies, η_{sys} and η_{PA}, respectively, when k increases from 0.14 to 0.44. As shown in Figs. 1 and 3, η_{sys} is defined as P_o/P_{dc}, i.e., dc-dc efficiency, and η_{PA} is $P_{Z_{in}}/P_{dc}$. Here the PA dc voltage, V_{dc}, is 20 V. Note similar results should be obtained for other permissible PA dc voltages when a same target region of the PA load is applied [refer to section III-B]. The experimental results of the conventional WPT system without the matching network are also given for comparison purposes. Note that gate drive loss is not included in the above efficiencies because it is relatively small, about 130 mW in measurements. The WPT system using the optimally designed matching network shows an obvious improvement in both the system and PA efficiencies over a wide range of k. The efficiencies for the k's around 0.2 are only slightly compromised. This result is natural because

the conventional design is the one optimized for $k=0.2$. The output power of the PA is shown in Fig. 8(c), which is again largely improved under different k's, particularly when k is large, i.e. a close coil distance. All the PA efficiencies and output power are higher than 85% and 8 W, respectively, which is consistent with the requirements when determining the target region in (23). Note that the trend of efficiencies in Fig. 8(a) and (b) is largely independent of a specific power level except the power is extremely low. The efficiencies at the same power level, 5 W, are also confirmed in experiments. Because the efficiency curves are almost identical with the ones in Fig. 8(a) and (b). For the sake of simplicity, they are not shown here. The improvement in THD in the input voltage of the coupling coils, $V_{Z_{in}}$, is even significant, as shown in Fig. 8(d). The average reduction of the THD is 77.5% over the k's.
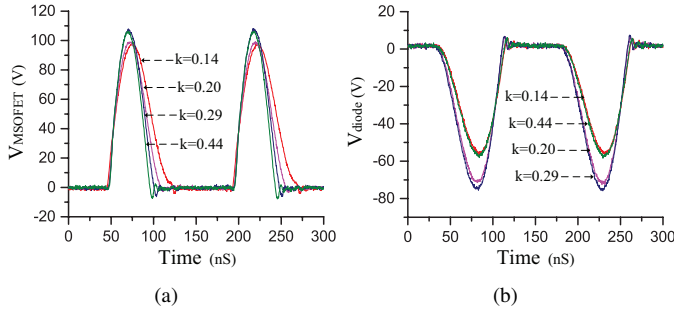
Fig. 9. Voltage waveforms. (a) MOSFET. (b) Rectifying diode.

Fig. 9 show voltage waveforms of the MOSFET and rectifying diodes when k changes. From Fig. 9(a), it can be seen that the Class E PA works close to its ZVS operation. In Fig. 9 (b), amplitude of rectifying diode voltage at $k=0.2$ and $k=0.29$ is higher due to the higher output power of the rectifier [refer to Fig. 8(c)]. The waveforms and harmonic contents of $v_{Z_{in}}$, the input voltage of the coupling coils, at $k=0.2$ are further shown in Fig. 10. The THD is significantly improved, less than one fifth of the previous THD in the conventional design. Thus the waveform of $v_{Z_{in}}$ is very close to the ideal sinusoidal one, which indicates lower EMI generation. The THD of output voltage of the original Class E PA (i.e., $V_{Z_{in}}$ and V_{Z_0} in the conventional and improved designs, respectively) is also confirmed in experiments. The THD is reduced from 52.9% to 16.1%. All the above experimental results convincingly show that the adding of the π matching network after the Class E PA and its optimized design improve both the efficiency and the output power of the PA and the overall WPT system, and also greatly help to suppress the harmonic contents.

For reference purposes, the efficiencies of the PA, rectifier, and WPT system are shown in Fig. 11(a) when the dc load R_L varies between 10–50 Ω. Note that the nominal R_L is 30 Ω. The efficiencies are comparable to those when k changes because the original target of the proposed design is to limit the variation of reflected impedance seen by the PA [see Fig. 5]. Besides the design methodology, new devices such as gallium nitride (GaN) MOSFETs could also possibly improve the system efficiency [28]. As shown in Fig. 11(b), the system efficiency and PA efficiency using GaN MOSFET
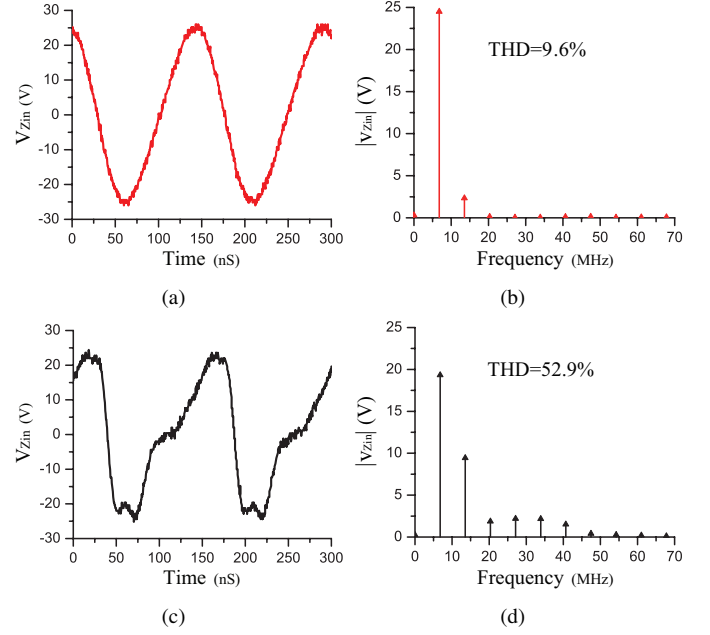
Fig. 10. Waveforms and harmonic contents of $v_{Z_{in}}$, the input voltage of the coupling coils, at $k=0.2$. (a) Waveform of $v_{Z_{in}}$ with matching network. (b) Harmonic contents of $v_{Z_{in}}$ with matching network. (c) Waveform of $v_{Z_{in}}$ without matching network. (d) Harmonic contents of $v_{Z_{in}}$ without matching network.

(GS66508T) show improvement compared with those using the Si MOSFET (SUD06N10), particularly when k is small. It is mainly because of fast switching and small on-resistance of the GaN MOSFET. In experiments, the nonlinear drain-source parasitic capacitance of GS66508T is estimated as 170 pF based on the datasheet and PA drain voltage at $k=0.2$, the nominal value in this paper. The parasitic capacitance is absorbed into the PA shunt capacitor, C_S (=262 pF). Since the PA drain voltage at $k=0.29$ and $k=0.44$ deviates from that at $k=0.2$ [refer to Fig. 9], the total shunt capacitance, C_S, at $k=0.29$ and $k=0.44$ becomes different with its original target value, 262 pF. Thus efficiency improvement using GaN MOSFET is not obvious at large k's such as $k=0.29$ and $k=0.44$, as shown in Fig. 11(b).
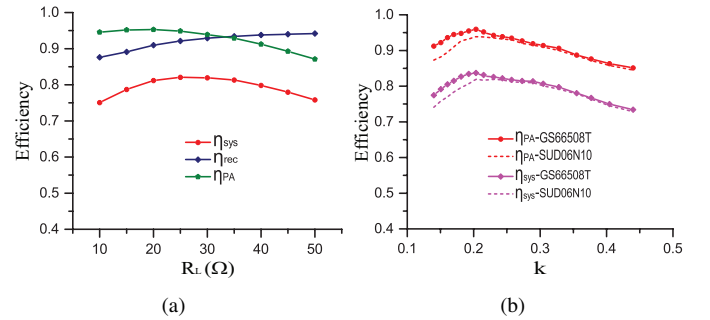
Fig. 11. Further experimental results. (a) Efficiencies under a varying R_L. (b) Efficiencies using GaN MOSFET (GS66508T).

V. CONCLUSIONS

This paper discusses improvements on the circuit and design methodology for a MHz WPT system using both Class E

PA and Class E full-wave rectifier. The purpose is to further enhance the performance of the WPT system, in terms of the efficiency/output power and the harmonic contents, when the mutual inductance coefficient, k, varies. The π matching network is newly added and designed (i.e., C_L and C_R) in such a way that the load of the PA, namely the input impedance of the matching network, always maintains within the desired range when the variation of k occurs, and at the same time minimizes the second-order harmonic in the input voltage of the coupling coils. The experimental results well validate the theoretical analysis and the design approach. A high efficiency and output power of the Class E PA and the overall system is achieved over a wide range of the mutual inductance, k from 0.14 to 0.44. In addition, the THD of the input voltage of the coupling coils is significantly reduced from 52.9% to 9.6%, which contributes to ease the EMI problem. The circuit and design improvements discussed in this paper could serve as a general and practical solution when building high performance MHz WPT systems.

References

[1] "Improving the effectiveness, flexibility and availability of spectrum for short range devices," in *Document RAG07-1/17-E, , Radiocommunication Advisory Group, International Telecommunication Union*, 2007.

[2] P. Raval, D. Kacprzak, and A. Hu, "Multiphase inductive power transfer box based on a rotating magnetic field," *IEEE Trans. Ind. Electron.*, vol. 62, no. 2, pp. 795–802, Feb. 2015.

[3] D. Ahn and S. Hong, "Wireless power transfer resonance coupling amplification by load-modulation switching controller," *IEEE Trans. Ind. Electron.*, vol. 62, no. 2, pp. 898–909, Feb. 2015.

[4] S.-J. Huang, T.-S. Lee, and T.-H. Huang, "Inductive power transfer systems for PT-based ozone-driven circuit with flexible capacity operation and frequency-tracking mechanism," *IEEE Trans. Ind. Electron.*, vol. 61, no. 12, pp. 6691–6699, Dec. 2014.

[5] V. Prasanth and P. Bauer, "Distributed IPT systems for dynamic powering: Misalignment analysis," *IEEE Trans. Ind. Electron.*, vol. 61, no. 11, pp. 6013–6021, Nov. 2014.

[6] D. Ahn and S. Hong, "Wireless power transmission with self-regulated output voltage for biomedical implant," *IEEE Trans. Ind. Electron.*, vol. 61, no. 5, pp. 2225–2235, May 2014.

[7] W. Zhong, C. Zhang, X. Liu, and S. Hui, "A methodology for making a three-coil wireless power transfer system more energy efficient than a two-coil counterpart for extended transfer distance," *IEEE Trans. Power Electron.*, vol. 30, no. 2, pp. 933–942, Feb. 2015.

[8] A. Kurs, A. Karalis, R. Moffatt, J. D. Joannopoulos, P. Fisher, and M. Soljačić, "Wireless power transfer via strongly coupled magnetic resonances," *science*, vol. 317, no. 5834, pp. 83–86, 2007.

[9] S. Hui, W. Zhong, and C. Lee, "A critical review of recent progress in mid-range wireless power transfer," *IEEE Trans. Power Electron.*, vol. 29, no. 9, pp. 4500–4511, Sep. 2014.

[10] M. Fu, T. Zhang, C. Ma, and X. Zhu, "Efficiency and optimal loads analysis for multiple-receiver wireless power transfer systems," *IEEE Trans. Microw. Theory Tech.*, vol. 63, no. 3, pp. 801–812, Mar. 2015.

[11] M. Pinuela, D. C. Yates, S. Lucyszyn, and P. D. Mitcheson, "Maximizing DC-to-load efficiency for inductive power transfer," *IEEE Trans. Power Electron.*, vol. 28, no. 5, pp. 2437–2447, May 2013.

[12] A. Sample, B. Waters, S. Wisdom, and J. Smith, "Enabling seamless wireless power delivery in dynamic environments," *Proc. IEEE*, vol. 101, no. 6, pp. 1343–1358, Jun. 2013.

[13] S.-H. Lee and R. D. Lorenz, "Development and validation of model for 95%-efficiency 220-w wireless power transfer over a 30-cm air gap," *IEEE Trans. Appl. Ind.*, vol. 47, no. 6, pp. 2495–2504, Nov. 2011.

[14] M. Fu, H. Yin, X. Zhu, and C. Ma, "Analysis and tracking of optimal load in wireless power transfer systems," *IEEE Trans. Power Electron.*, vol. 30, no. 7, pp. 3952–3963, Jul. 2015.

[15] M. Fu, C. Ma, and X. Zhu, "A cascaded boost-buck converter for high efficiency wireless power transfer systems," *IEEE Trans. Ind. Informat.*, vol. 10, no. 3, pp. 1972–1980, Aug. 2014.

[16] S. Aldhaher, P.-K. Luk, and J. F. Whidborne, "Electronic tuning of misaligned coils in wireless power transfer systems," *IEEE Trans. Power Electron.*, vol. 29, no. 11, pp. 5975–5982, Nov. 2014.

[17] S. Aldhaher, P.-K. Luk, K. El Khamlichi Drissi, and J. Whidborne, "High-input-voltage high-frequency Class E rectifiers for resonant inductive links," *IEEE Trans. Power Electron.*, vol. 30, no. 3, pp. 1328–1335, Mar. 2015.

[18] P.-K. Luk, S. Aldhaher, W. Fei, and J. Whidborne, "State-space modeling of a Class E^2 converter for inductive links," *IEEE Trans. Power Electron.*, vol. 30, no. 6, pp. 3242–3251, Jun. 2015.

[19] S. Liu, M. Liu, M. Fu, C. Ma, and X. Zhu, "A high-efficiency Class-E power amplifier with wide-range load in WPT systems," in *Proc. Wireless Power Transfer Conference (WPTC),2015 IEEE*, Boulder,Colorado,USA, May 2015, pp. 1–3.

[20] M. Liu, M. Fu, and C. Ma, "Parameter design for a 6.78-MHz wireless power transfer system based on analytical derivation of Class E current-driven rectifier," *IEEE Trans. Power Electron.*, vol. 31, no. 6, pp. 4280–4291, Jun. 2016.

[21] S. Aldhaher, P.-K. Luk, A. Bati, and J. Whidborne, "Wireless power transfer using Class E inverter with saturable DC-feed inductor," *IEEE Trans. Ind. Appl.*, vol. 50, no. 4, pp. 2710–2718, Jul. 2014.

[22] R. E. Zulinski and K. J. Grady, "Load-independent class e power inverters. i. theoretical development," *IEEE Trans. Circuits Syst.*, vol. 37, no. 8, pp. 1010–1018, Aug. 1990.

[23] L. Roslaniec and D. J. Perreault, "Design of variable-resistance Class E inverters for load modulation," in *2012 IEEE Energy Conversion Congress and Exposition (ECCE)*, Raleigh,North Carolina,USA, Sep. 2012, pp. 3226–3232.

[24] J. Park, Y. Tak, Y. Kim, Y. Kim, and S. Nam, "Investigation of adaptive matching methods for near-field wireless power transfer," *IEEE Trans. Antennas Propag.*, vol. 59, no. 5, pp. 1769–1773, May 2011.

[25] T. C. Beh, M. Kato, T. Imura, S. Oh, and Y. Hori, "Automated impedance matching system for robust wireless power transfer via magnetic resonance coupling," *IEEE Trans. Ind. Electron.*, vol. 60, no. 9, pp. 3689–3698, Sep. 2013.

[26] A. Reatti, M. Kazimierczuk, and R. Redl, "Class E full-wave low dv/dt rectifier," *IEEE Trans.Circuits Syst. I, Fundam. Theory Appl.*, vol. 40, no. 2, pp. 73–85, Feb. 1993.

[27] M. Albulet, *RF power amplifiers*. SciTech Publishing, 2001.

[28] J. Choi, D. Tsukiyama, Y. Tsuruda, and J. Rivas, "13.56 MHz 1.3 kW resonant converter with GaN FET for wireless power transfer," in *2015 IEEE Wireless Power Transfer Conference (WPTC)*, Boulder,Colorado,USA, May 2015, pp. 1–4.
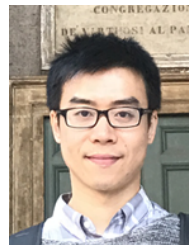
Ming Liu (S'15) received the B.S. degree from SiChuan University, Sichuan, China, in 2007, and the M.S. degree from the University of Science and Technology Beijing, Beijing, China, in 2011, both in mechatronic engineering. He is currently working toward the Ph.D. degree in electrical and computer engineering at the University of Michigan-Shanghai Jiao Tong University Joint Institute, Shanghai Jiao Tong University, Shanghai, China.

His research interests include high frequency power electronic circuits such as high frequency resonant converters and megahertz wireless power transfer systems, general power electronics and applications, circuit-level and system-level optimization.

Shuangke Liu (S'15) received the B.S. degree in electronics and information engineering from Xidian University, Xian, China, in 2013. She is currently working toward the Ph.D. degree in electrical and computer engineering at the University of Michigan-Shanghai Jiao Tong University Joint Institute, Shanghai Jiao Tong University, Shanghai, China.

Her research interests include optimal design of high-frequency wireless power transfer system and RF/microwave circuit design.

Chengbin Ma (M'05) received the B.S. (Hons.) degree in industrial automation from East China University of Science and Technology, Shanghai, China, in 1997, and the M.S. and Ph.D. degrees in electrical engineering from The University of Tokyo, Tokyo, Japan, in 2001 and 2004, respectively.

He is currently an associate professor of electrical and computer engineering at University of Michigan-Shanghai Jiao Tong University Joint Institute, Shanghai Jiao Tong University, Shanghai, China. Between 2006 and 2008, he held a postdoctoral position with the Department of Mechanical and Aeronautical Engineering, University of California Davis, California, USA. From 2004 to 2006, he was a R&D researcher with Servo Laboratory, Fanuc Limited, Yamanashi, Japan. He is an associate editor of the IEEE Transactions on Industrial Informatics. His research interests include networked energy systems, wireless power transfer, and mechatronic control.